

Local thermal resonance control of GaInP photonic crystal membrane cavities using ambient gas cooling

Sergei Sokolov,^{1, a)} Jin Lian,¹ Emre Yüce,¹ Sylvain Combrié,² Gaelle Lehoucq,² Alfredo De Rossi,² and Allard P. Mosk¹

¹⁾Complex Photonic Systems (COPS), MESA+ Institute for Nanotechnology, University of Twente, 7500 AE Enschede, The Netherlands

²⁾Thales Research & Technology, Route Départementale 128, 91767 Palaiseau, France

(Dated: 7 December 2024)

We perform a spatially dependent tuning of a GaInP photonic crystal cavity using a continuous wave violet laser. Local tuning is obtained by laser heating of the photonic crystal membrane. The cavity resonance shift is measured for different pump positions and for two ambient gases: He and N₂. The use of high-conducting gas in combination with low-conducting semiconductor leads to a resonance control with a spatial resolution better than 4 μ m.

Photonic crystal (PhC) cavities are widely studied because of their fascinating applications¹. Arrays of PhC cavities can form coupled resonator optical waveguides (CROW), which are very promising for slow light applications² and the study of light localization³. Various fabrication imperfections can cause disorder in a CROW structure which leads to detuning of cavities from the intended resonance and reduces the waveguide performance. Tuning each cavity independently can restore cavities back into the resonance and counteract disorder. There is a variety of methods to change the refractive index of PhC cavity: using free-carriers⁴, using Kerr effect⁵, using heat^{6,7}, by oxidation⁸⁻¹⁰, and chemically¹¹. Of these methods, thermal tuning is easy, reversible and can give steady-state control of resonance properties of the system. However due to heat diffusion, thermal control of one cavity will affect the neighbor cavities. The heat spread in the sample is determined by the material of the sample and by the surrounding media, therefore one can expect that by selecting a certain combination of the sample material and the ambient media the reduction of the heat spread inside the PhC can be achieved.

In this work we use the semiconductor alloy Ga_{0.51}In_{0.49}P as a sample material and two gases, nitrogen and helium, as surrounding media. Ga_{0.51}In_{0.49}P has a thermal conductivity¹² of 4.9 W/(m·K) which is quite small in comparison to other semiconductor materials¹³. The larger the thermal conductivity of the ambient gas the faster the heat exchange between the gas and the sample. The thermal conductivity of gases usually is assumed to be negligible compared to semiconductors. Helium has a high thermal conductivity¹⁴ of 0.153 W/(m·K), which is more than 6 times higher than nitrogen¹⁴(0.024 W/(m·K)) and only 32 times smaller than that of Ga_{0.51}In_{0.49}P. Therefore the combination of Ga_{0.51}In_{0.49}P and He should increase the thermal ex-

change efficiency and decrease the FWHM of a heat distribution in comparison with other materials. To investigate the heat spread in PhC membranes we measured the response of the H0 cavity resonance to spatially scanned continuous wave (CW) pump light. The

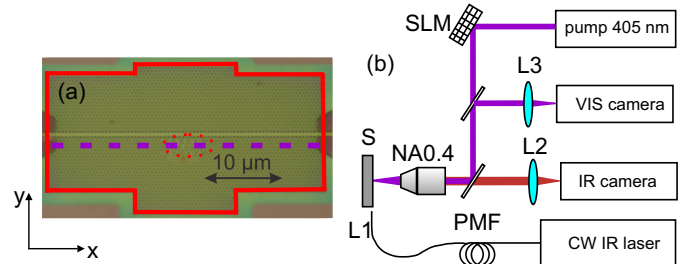


FIG. 1. (a) Optical microscope image of a GaInP PhC with an H0 cavity in the center. The cavity is indicated with the red dotted ellipse. The dashed purple line indicates the pump movement direction. (b) The pump-probe setup. The pump with a wavelength 405 nm was focused on a sample S using an objective. The sample's surface is imaged on a VIS camera using lens L3. The IR probe light was focused on a mode converter using lens L1 with NA 0.55. The vertically scattered IR light is collected with the same objective and imaged on an IR CCD using lens L2.

PhC H0 nanocavity is implemented in a triangular lattice of air holes with a period $a=505$ nm and hole radius 0.24 a . The hole shift for the H0 cavity is 0.16 a . A subharmonic hole structure is induced to enhance radiation from the cavity in a vertical direction¹⁵. The cavity is made of an air-suspended membrane of Ga_{0.51}In_{0.49}P with a thickness of 180 nm. The membrane is covered with 30 nm of SiN on the top using a PECVD technique. The detailed description of the fabrication method can be found in Ref. 16. A microscope picture of the cavity with the surrounding PhC is presented in Fig. 1a. The cavity is close to the center of the membrane and the IR light is evanescently coupled through a PhC waveguide. Mode converters are fabricated at the end of the waveguide to decrease the Fabri-Perot interference in the

^{a)}s.sokolov@utwente.nl; <http://cops.nano-cops.com>

waveguide and to increase the coupling efficiency¹⁷.

The setup used in the experiment is shown in Fig. 1b. The CW IR laser probe light was coupled to the PhC waveguide using a polarization maintaining lensed fiber with NA of 0.55. The out-of-plane scattered light was collected using a 0.4 NA objective and imaged on an IR CCD camera using lens L2. The total magnification of the system is 50x. We recorded spectra by changing the wavelength of the IR laser and taking IR camera snapshots for each wavelength. The oxygen concentration was monitored during the experiment and it was decreased down to 0.025% to suppress oxidation effects observed in other works⁸⁻¹⁰. The gas pressure in a chamber was close to the ambient air pressure. The thermal tuning was performed using a 405 nm CW diode laser light source, which was focused onto the surface of the sample into a tight spot with a FWHM of 0.9 μm using the same objective. The surface of the sample with the pump spot was also imaged with a visible range camera using lens L3 with the system magnification of 27x. The position of the pump spot was controlled using a spatial light modulator. The pump spot was moved along the purple line (see Fig. 1a) and the resonance spectrum of the cavity was measured for a number of pump positions. Any effects of slow oxidation or water coverage are eliminated by alternating between reference spectra (without pump laser) and signal spectra (with pump).

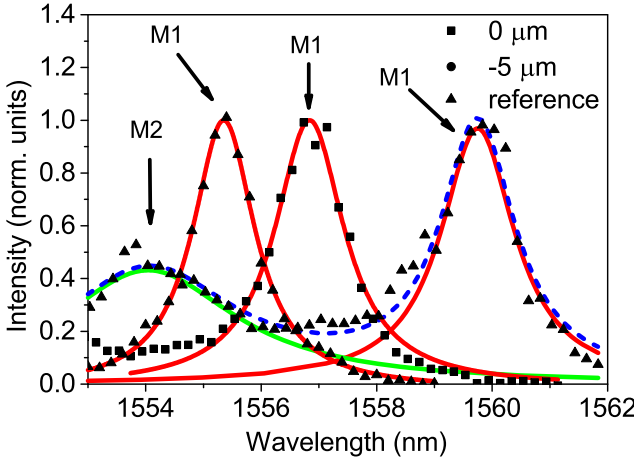


FIG. 2. Spectra obtained from the out-of-plane scattered light for untuned case and for pump positions on top of the cavity and 5 μm away from the center of the cavity in N₂. Color lines represent Lorentzian fits.

Reference resonance spectra and tuned spectra for pump positions of 0, -5 μm relatively to the center of the cavity in case of nitrogen are presented in Fig. 2. In general the closer the pump spot is placed to a cavity the stronger the redshift should be, due to the better overlap of the temperature profile and a cavity mode profile. There are two resonance modes observed: the high-Q low-frequency one (M1) and the low-Q high-frequency M2. Both resonances have distinct Lorentzian shape and the quality factor of about 1000 and 300 are estimated

for modes M1 and M2 correspondingly. The calculated loaded Q-factor of the mode M1 is about 2500, because the cavity is designed to be overcoupled. Resonance M2 corresponds to a higher order mode which is predicted from calculations. Mode M1 is much brighter than mode M2. Also these two modes have slightly different spatial positions, and pump light was focused on the spatial position of the mode M1. We use the frequency shift of mode M1 to determine the spatially dependent cavity response to the pump placed at a certain position. We note that apart from the redshift we saw the reduction of the intensity of the out-of-plane scattered light at pump positions close to the cavity. We surmise that this might happen due to perturbation of the subharmonic structure.

The pump power incident on the sample is 110 μW in N₂ atmosphere. The spatial response curve for N₂ atmosphere is presented on Fig. 3a. The maximum redshift is 4.5 nm, which was used for normalizing the graph. The FWHM is equal to 5 μm . In He atmosphere a pump spot

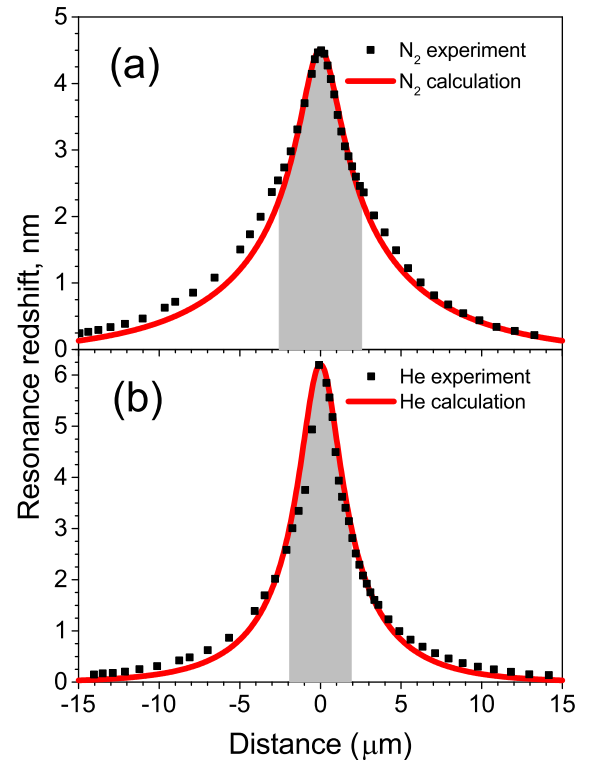


FIG. 3. Redshifts of the cavity resonance and cavity excess temperatures for different pump positions with nitrogen (a) and helium (b) as an ambient gas. Red curves represent the redshift calculated according to the model. From one measurement to another we observed an error less than 3% of the shift for N₂, and less than 1% for He.

of 220 μW was used to tune cavity (see Fig. 3b). The maximum observed redshift is 6.2 nm and the FWHM of the curve is 3.5 μm . As a result of the high thermal conductivity of the He, both the redshift (normalized to power) and the FWHM are smaller by 30%, compared to N₂. Decreased FWHM should reduce the thermal crosstalk

between cavities in a CROW.

We perform our numerical calculations to model the resonance wavelength change of the cavity for different pump positions taking into account all experimental conditions. It is known that for small perturbations of refractive index the wavelength change can be expressed in the following way¹⁸:

$$\Delta\lambda = \frac{\lambda}{\langle n \rangle} \frac{dn}{dT} \frac{\int \Delta T(\mathbf{r} - \mathbf{r}_0) \epsilon(\mathbf{r}) |\mathbf{E}(\mathbf{r})|^2 d^3r}{\int \epsilon(\mathbf{r}) |\mathbf{E}(\mathbf{r})|^2 d^3r}, \quad (1)$$

where ΔT is a local temperature variation in a PhC membrane, $\epsilon(\mathbf{r}) |\mathbf{E}(\mathbf{r})|^2$ is mode profile of the cavity, $\epsilon(\mathbf{r})$ is a dielectric constant of a membrane material, $\frac{dn}{dT}$ is a linear coefficient of the refractive index temperature response, \mathbf{r}_0 is position of the pump and $\langle n \rangle$ is an averaged refractive index of the membrane material. The mode profile was calculated using the MEEP package¹⁹. Temperature distributions are calculated in COMSOL using a steady state heat diffusion model with a constant source term assuming that thermal conductivities are not temperature dependent within the relevant temperature range:

$$\kappa(x, y, z) \nabla^2 T(x, y, z) + Q(x, y, z) = 0, \quad (2)$$

where $\kappa(x, y, z)$ is thermal conductivity and Q is a source term inside the membrane written as a sum of two terms $Q = Q_{excess} + Q_{recomb}$, due to the excess energy of the carriers and their recombination respectively.

We observe the photoluminescence (PL) of GaInP at 670 nm caused by the pump light. The bandgap of GaInP is 1.85 eV and the energy of a photon with wavelength 405 nm is 3.06 eV. The excess energy term (Q_{excess}) has the size of the pump spot 0.9 μm and corresponds to 40% of the initial power²⁰. The recombination term (Q_{recomb}) has the size of the PL, which is 1.2 μm , and it takes 60% of the photon energy. We assume that all absorbed light is converted into heat, because the estimated radiative carrier recombination efficiency is less than 1%²¹.

Both terms are weighted and described as:

$$Q(x, y, z) = \frac{P(1 - R)}{2\pi\sigma^2} \alpha e^{-(x^2 + y^2)/2\sigma^2} e^{-\alpha z}. \quad (3)$$

Here R is a reflection coefficient of the membrane estimated to be 9.5%, σ is standard deviation of the Gaussian distribution, α is the absorption coefficient of GaInP, P is the total power of the pump beam. The size of the air gap between the membrane and GaAs substrate for our samples is equal to 1.5 μm , the size of the air layer above the membrane was taken to be 10 μm . All external boundaries are Dirichlet type, assumed to have fixed temperature $T=293.15$ K. The photonic crystal is assumed to be a rectangle with sides of 40 and 20 μm . Dirichlet boundaries are considered because the membrane is surrounded from four sides by the bulk material, which acts like a perfect heat sink. Thermal conductivities for gases were taken from Ref. 14,22. The coating layer made of SiN has a thermal conductivity²³ of 24.5 W/(m·K). The

thermal conductivity of the membrane was taken as volume averaged between holes of the PhC lattice and two layers of SiN and GaInP. The absorption of SiN at 405 nm is negligible, and the light absorption coefficient²⁴ of $\text{Ga}_{0.51}\text{In}_{0.49}\text{P}$ is $24.5 (\mu\text{m})^{-1}$. That means that nearly all pump light is absorbed by the GaInP membrane. The numerical thermal profile can be calculated without any free parameters. The only parameter which is unknown for the redshift calculation is the thermal coefficient of the refractive index $\frac{dn}{dT}$ for $\text{Ga}_{0.51}\text{In}_{0.49}\text{P}$.

The calculation results are presented in Fig. 3a,b. The calculated curve shows an excellent agreement with the experiment for both nitrogen and helium. The maximum excess temperature in case of nitrogen atmosphere is 29 K, and in case of He it is 37 K, so the ratio of these two values normalized to the incident power is equal to 0.63 which is extremely close to the experimental ratio of redshifts: 0.69. From Fig. 3 we also estimate so far unknown the temperature coefficient of the refractive index of GaInP. We obtain $3 \times 10^{-4}\text{K}^{-1}$ from experiment with N₂ and $3.2 \times 10^{-4}\text{K}^{-1}$ for He. Both values are comparable to the literature value for GaP¹³.

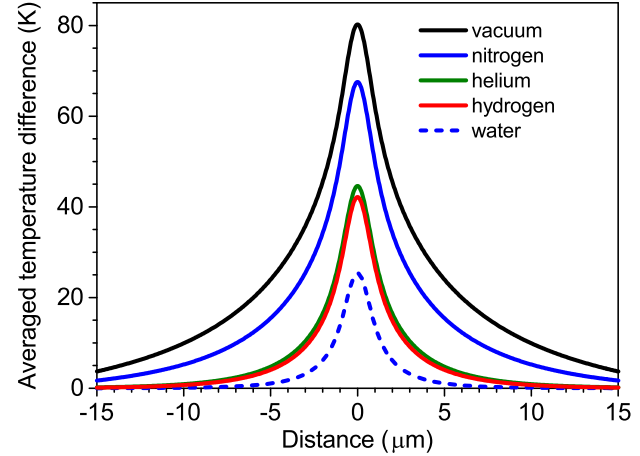


FIG. 4. X-axis cross-section of the calculated temperature distribution for different ambient media. The temperature is averaged over membrane thickness with the pump placed in the center of the cavity. The power of the pump light is equal to 220 μW .

From time-dependent simulations we estimate that 10% to 90% temperature rise time in case of nitrogen atmosphere is about 6 μs , but in case of helium it is about 2 μs . Therefore, helium not only helps to increase the spatial resolution of thermal tuning but also it makes it about three times faster.

Instead of helium one could in principle use materials with higher thermal conductivity. On the Fig. 4 calculated temperature distributions inside PhC membrane along the central line (see Fig. 1) with a pump placed in the center are presented. Thermal conductivity of H is 20% larger than for He, so the difference between these two cases is not significant. The widest temperature distribution is in case of vacuum, because there is no heat

exchange with ambient media. Water has thermal conductivity 4 times higher than He, which results in a great difference in a temperature distribution. We note that low refractive index liquids like acetone, isopropanol and etc., have thermal conductivity comparable to the one of He. Using liquids for heat exchange will completely change the optical properties of the sample, therefore using gases with high thermal conductivity is a great tool to reduce heat spread without changing sample's optical properties.

The general tendency of FWHM and peak averaged excess temperature of the temperature profile is presented on Fig. 5. In case of low thermal conductivities heat tends

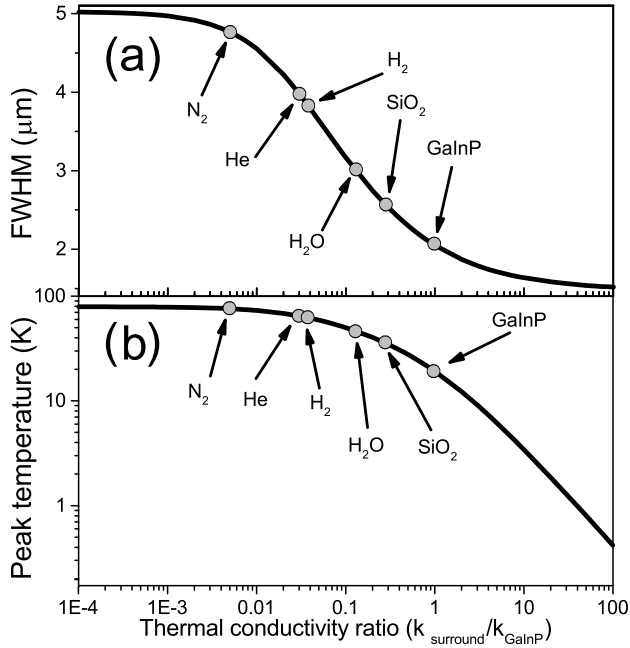


FIG. 5. Calculated FWHM (a) and peak excess temperature (b) of averaged temperature differences for different thermal conductivity ratios of surrounding media and $\text{Ga}_{0.51}\text{In}_{0.49}\text{P}$. Some well-known material are marked with circles and arrows. The power of the pump light is equal to $220 \mu\text{W}$.

to diffuse inside the membrane rather than towards the surrounding, therefore FWHM and peak excess temperature reaches largest values of $5 \mu\text{m}$ and 79 K . For large thermal conductivities of the surrounding media the heat exchange between the membrane and the media is fast, which means that the large part of the heat diffuses into the ambient media reducing FWHM and peak temperature. FWHM tends about $1.5 \mu\text{m}$ and peak excess temperature reaches 0 K for large thermal conductivities.

In conclusion, we measured the spectral tuning curve of a thermally tuned cavity for different surrounding media and found an excellent agreement between experiment and our numerical calculations. Our results and our calculations are extremely useful for applications like thermal control of CROWs where heat spread should be

minimized. Also our temperature distribution calculations can help to select an ambient material for other applications which involve local laser heating.

The authors would like to thank Henri Thyrrestrup and Willem Vos for helpful discussions and advices and Cornelis Harteveld for technical support. This work was supported by European Research Council (project No. 279248).

- ¹A. B. Matsko, *Practical Applications of microresonators in optics and photonics* (CRC Press, 2009).
- ²N. Matsuda, E. Kuramochi, H. Takesue, and M. Notomi, Opt. Lett. **39**, 2290 (2014).
- ³S. Mookherjea, J. S. Park, S. Yang, and P. R. Bandaru, Nat. Photonics **2**, 90 (2008).
- ⁴C. Husko, A. D. Rossi, S. Combrié, Q. V. Tran, and F. R. et al., Appl. Phys. Lett. **94**, 021111 (2009).
- ⁵E. Yüce, G. Ctistis, J. Claudon, E. Dupuy, R. D. Buijs, B. de Ronde, A. P. Mosk, J.-M. Gérard, and W. L. Vos, Opt. Lett. **938**, 12480 (2013).
- ⁶M. Notomi, A. Shinya, S. Mitsugi, G. Kira, E. Kuramochi, and T. Tanabe, Opt. Expr. **4**, 2678 (2005).
- ⁷J. Pan, Y. Huo, K. Yamanaka, S. Sandhu, L. S. R. Timp, M. L. Povinelli, S. Fan, and J. S. Harris, Appl. Phys. Lett. **92**, 103114 (2008).
- ⁸C. J. Chen, J. Zheng, T. Gu, J. F. McMillan, M. Yu, G. Lo, D. Kwong, and C. W. Wong, Opt. Expr. **19**, 2678 (2011).
- ⁹H. S. Lee, S. Kiravittaya, S. Kumar, J. D. Plumhof, L. Balet, L. H. Li, M. Francardi, A. Gerardino, A. Fiore, A. Rastelli, and O. G. Schmidt, Opt. Expr. **95**, 191109 (2009).
- ¹⁰F. Riboli, N. Caselli, S. Vignolini, F. Intonti, K. Vynck, P. Barthelemy, A. Gerardino, L. Balet, L. Li, A. Fiore, M. Gurioli, and D. Wiersma, Nat. Mater. **13**, 720 (2014).
- ¹¹K. Hennessy, A. Badolato, A. Tamboli, P. M. Petroff, E. Hu, M. Atature, J. Dreiser, and A. Imamoglu, Appl. Phys. Lett. **87**, 021108 (2005).
- ¹²S. Adachi, J. Appl. Phys. **102**, 063502 (2007).
- ¹³M. Levinshtein, S. Rumyantsev, and M. Shur, *Handbook series on Semiconductor Parameters*, Vol. 1 (Wold Scientific, 1996).
- ¹⁴H. Anderson, *A Physicist's Desk Reference* (American institute of physics, NY, 1989).
- ¹⁵N. Tran, S. Combrié, P. Colman, A. D. Rossi, and T. Mei, Phys. Rev. B **82**, 075120 (2010).
- ¹⁶S. Combrié, S. Bansropun, M. Lecomte, O. Parillaud, and S. C. et al., J. Vac. Sci. Technol. B **23**, 1521 (2005).
- ¹⁷Q. Tran, S. Combrié, P. Colman, and A. D. Rossi, Appl. Phys. Lett. **95**, 061105 (2009).
- ¹⁸J. Joannopoulos, S. G. Johnson, J. N. Winn, and R. D. Meade, *Photonic Crystals Molding the flow of light* (PRINCETON UNIVERSITY PRESS, 2008).
- ¹⁹A. F. Oskooi, D. Roundy, M. Ibanescu, P. Bermel, J. D. Joannopoulos, and S. G. Johnson, Comp. Phys. Comm. **181**, 687 (2010).
- ²⁰Carrier thermalisation term has 40% of the energy because the ration of the GaInP bandgap to the pump photon energy is 0.4.
- ²¹The carrier recombination efficiency is estimated as a ratio of counts of the PL intensity to counts of the reflection of the pump laser light from the sample surface.
- ²²Y. S. Touloukian, P. Liley, and S. C. Saxena, *Thermophysical properties of matter*, Vol. 3 (IFI/PLENUM, New York-Washington, 1970).
- ²³MIT material property database, <http://www.mit.edu/6.777/matprops/matprops.htm>.
- ²⁴M. Schubert, V. Gottschalch, C. M. Herzinger, H. Yao, and P. G. Snyder, J. Appl. Phys. **77**, 3416 (1995).